Physics Letters B 763 (2016) 108–113

Contents lists available at ScienceDirect

Physics Letters B

www.elsevier.com/locate/physletb

Shape coexistence from lifetime and branching-ratio measurements in ^{68,70}Ni

B.P. Crider [a,*], C.J. Prokop [a,b], S.N. Liddick [a,b], M. Al-Shudifat [c], A.D. Ayangeakaa [d], M.P. Carpenter [d], J.J. Carroll [e], J. Chen [a], C.J. Chiara [f], H.M. David [d,1], A.C. Dombos [a,g], S. Go [c], R. Grzywacz [c,h], J. Harker [d,i], R.V.F. Janssens [d], N. Larson [a,b], T. Lauritsen [d], R. Lewis [a,b], S.J. Quinn [a,g], F. Recchia [j], A. Spyrou [a,g], S. Suchyta [k], W.B. Walters [i], S. Zhu [d]

[a] National Superconducting Cyclotron Laboratory, Michigan State University, East Lansing, MI 48824, USA
[b] Department of Chemistry, Michigan State University, East Lansing, MI 48824, USA
[c] Department of Physics and Astronomy, University of Tennessee, Knoxville, TN 37996, USA
[d] Physics Division, Argonne National Laboratory, Argonne, IL 60439, USA
[e] U.S. Army Research Laboratory, Adelphi, MD 20783, USA
[f] Oak Ridge Associated Universities Fellowship Program, U.S. Army Research Laboratory, Adelphi, MD 20783, USA
[g] Department of Physics, Michigan State University, East Lansing, MI 48824, USA
[h] Physics Division, Oak Ridge National Laboratory, Oak Ridge, TN 37830, USA
[i] Department of Chemistry and Biochemistry, University of Maryland, College Park, MD 20742, USA
[j] Dipartimento di Fisica e Astronomia, Università degli Studi di Padova, I-35131 Padova, Italy
[k] Department of Nuclear Engineering, University of California Berkeley, Berkeley, CA 94720, USA

ARTICLE INFO

Article history:
Received 15 August 2016
Accepted 11 October 2016
Available online 15 October 2016
Editor: D.F. Geesaman

ABSTRACT

Shape coexistence near closed-shell nuclei, whereby states associated with deformed shapes appear at relatively low excitation energy alongside spherical ones, is indicative of the rapid change in structure that can occur with the addition or removal of a few protons or neutrons. Near ^{68}Ni ($Z = 28$, $N = 40$), the identification of shape coexistence hinges on hitherto undetermined transition rates to and from low-energy 0^+ states. In ^{68,70}Ni, new lifetimes and branching ratios have been measured. These data enable quantitative descriptions of the 0^+ states through the deduced transition rates and serve as sensitive probes for characterizing their nuclear wave functions. The results are compared to, and consistent with, large-scale shell-model calculations which predict shape coexistence. With the firm identification of this phenomenon near ^{68}Ni, shape coexistence is now observed in all currently accessible regions of the nuclear chart with closed proton shells and mid-shell neutrons.

Nuclei exhibit shell structure, a characteristic of finite, many-body quantum systems. The evidence for shell structure is extensive, with one example being the sudden drop in nucleon separation energy that occurs at so-called magic numbers 2, 8, 20, 28, 50, 82, and 126 [1]. Nuclei near closed shells are typically spherical in their lowest-energy states. Levels associated with the excitation of nucleons across shell gaps are thought to be located at the high excitation energies corresponding to the size of the gaps. However, residual proton-neutron interactions can stabilize excitations across the closed shells while driving the nucleus towards deformation. As a result, low-lying collective bands sometimes appear alongside the spherical states [2]. This shape coexistence is observed in the heavier-mass Pb [3] and Sn regions [4–7] and has recently been proposed for the neutron-rich Ni region [8–12]. The excitation energy of the deformed, coexisting states decreases when moving away from a shell closure towards mid-shell, where it minimizes. Examples have been extensively documented in even-Pb isotopes, centered on $^{186}_{82}Pb_{104}$ [2], and even-Sn isotopes, centered on $^{116}_{50}Sn_{66}$ [13], both located near the middle of the $N = 82$–126 and $N = 50$–82 shells, respectively. However, these trends are apparent only after the individual states in various nuclei are grouped together according to their underlying configurations. To this end, electromagnetic transition rates and branching ratios are important

* Corresponding author.
E-mail address: crider@nscl.msu.edu (B.P. Crider).
[1] Present address: GSI Helmholtzzentrum für Schwerionenforschung GmbH, 64291 Darmstadt, Germany.

http://dx.doi.org/10.1016/j.physletb.2016.10.020

experimental probes of nuclear wave functions, enabling proper association of the levels of interest.

Confirming shape coexistence in neutron-rich Ni isotopes would establish the phenomenon in all proton shells midway between two neutron magic numbers. This would, in turn, enable a-priori predictions of the regions of N and Z where shape coexistence will manifest itself and have implications for other fields. Astrophysical abundance predictions for explosive stellar processes such as the rapid neutron capture process (r process), which proceeds through very neutron-rich nuclei, are sensitive to a number of nuclear decay properties. Shape coexistence can bring about rapid changes in the ground-state properties of exotic nuclei over a relatively small span of either neutron or proton numbers and significantly affect half-lives, as has already been demonstrated in the Zr-Mo region [14].

In even-even nuclei, a signature of shape coexistence is the presence of multiple, low-lying excited 0^+ states. Three low-energy 0^+ levels are known in ^{68}Ni: the ground state, the first excited state at 1604 keV [10,15,16], and a 0^+ level at 2511 keV [17,18]. These three 0^+ levels have been associated with spherical, oblate, and prolate shapes, respectively, based on comparisons with large scale shell-model calculations [10,19,16,20]. The establishment and characterization of shape coexistence within a nucleus requires going beyond energy and spin-parity assignments of the nuclear levels to, for example, determining absolute transition strengths and mixing parameters. Information on reduced transition probabilities acts as a fingerprint of different nuclear configurations and the degree of overlap between the nuclear wave functions involved [2]. Along the same lines, electric monopole ($E0$) transition strengths between 0^+ states reflect the mixing of configurations with different mean-square charge radii. Large-scale, shell-model calculations indicate the importance of configuration mixing in understanding the low-energy level structure of ^{68}Ni [15,18,12,21,22,19]. Herein, we report on the 0_3^+ level lifetime and the $2_1^+ \rightarrow 0_2^+$ branching ratio which, when combined with the $E0$ transition strength, provide a clear signature for coexisting spherical and deformed configurations. Furthermore, this first observation of the weak $2_1^+ \rightarrow 0_2^+$ branch enables the determination of the ratio of electric quadrupole transition probabilities from the 2_1^+ state to both the 0_2^+ and the 0_1^+ levels. Within a two-level mixing model, this yields the first fully quantitative picture of shape coexistence in ^{68}Ni. This new result matches theoretical predictions without the need for any additional assumptions other than those implicit to the two-state mixing model.

Upon addition of just two neutrons leading to ^{70}Ni, the expectations for shape coexistence differ. Some models predict spherical-prolate shape coexistence [10,19,16] while others predict no shape coexistence at all [23–25]. The recent observation of a tentative 0^+ state at 1567 keV in ^{70}Ni [11] suggested a drop in excitation energy of the prolate potential minimum, in line with theoretical expectations for the neutron-rich, even-Ni isotopes. The measurement of the 0_2^+ level lifetime in ^{70}Ni, also reported here, results in a transition strength comparable to that observed for the prolate 0_3^+ state in ^{68}Ni.

An experiment was performed at the National Superconducting Cyclotron Laboratory (NSCL) to study low-lying 0^+ levels in ^{68,70}Ni. Radioactive ions of ^{68}Fe and ^{70}Co were produced through fragmentation of a ^{76}Ge primary beam ($E = 130$ MeV/A) on a ^{9}Be target. The A1900 spectrometer [26] was employed to separate fragments of interest from other reaction products. These fragments were transmitted to the experimental end station, which consisted of three silicon PIN detectors located approximately 1 m upstream of a central implantation scintillator. Incident ions were identified on an event-by-event basis using $\Delta E - TOF$ techniques and deposited 2–3 mm deep in a 5.2 cm $\times$ 5.2 cm $\times$ 1 cm thick pixelated, fast plastic scintillator coupled to a position-sensitive photomultiplier tube [27]. The position and arrival time of each implanted ion was recorded and correlated with subsequent β-decay electrons using spatial and temporal information. The β decay of ^{68}Fe was used to selectively populate the low-spin isomer in ^{68}Co, which subsequently fed states in ^{68}Ni. The β decay of ^{70}Co was used to investigate excited states of ^{70}Ni. The central implantation scintillator was surrounded by two ancillary photon detection arrays. Ten $LaBr_3$(Ce) detectors were placed in two annular rings surrounding the central implantation scintillator and the Segmented Germanium Array (SeGA) [28], with 16 high-purity germanium detectors, was arranged into two concentric rings of eight detectors each. Beta-delayed γ rays measured in the two ancillary arrays were observed within two seconds of the arrival of a ^{70}Co ion or four seconds of a ^{68}Fe ion. All detectors were read out with the NSCL digital data acquisition system [29]. Absolute γ-ray efficiencies were determined with a calibrated ^{154,155}Eu source and matched to GEANT4 [30] simulations.

Timing walk corrections between the implantation scintillator and the $LaBr_3$(Ce) detectors were determined using a ^{60}Co source and a technique described in Ref. [31]. The time properties of the system were verified by gating on the 1077-keV, 2_1^+ level in ^{68}Zn ($t_{1/2} = 1.6$ ps), a long-lived daughter product of ^{68}Fe. The short half-life is below the experimental sensitivity and the intrinsic time resolution of the system is shown in Fig. 1(a).

Longer level lifetimes will appear as a shift in the centroid of the prompt response or as a tail at larger time differences. The time-difference spectrum of Fig. 1(b) was created by gating around the $6_1^+ \rightarrow 4_1^+$ 448-keV, ^{70}Co, β-delayed γ ray in the $LaBr_3$(Ce) detectors. The profile of the background was obtained from an energy gate placed below the 448-keV peak (to avoid potential contamination from the 478-keV γ ray) and is indicated by the dashed line in Fig. 1(b). The best-fit lifetime in the convolution of Gaussian and exponential functions is shown with the thick solid line in Fig. 1(b) and resulted in a half-life of $t_{1/2} = 1.04(6)$ ns for the 6^+ state, in good agreement with the $t_{1/2} = 1.05(3)$ ns value reported by Mach *et al.* [32].

A half-life of 0.57(5) ns for the 0_3^+ state in ^{68}Ni was extracted with a gate on the 478-keV, $0_3^+ \rightarrow 2_1^+$ γ ray using the decay curve presented in Fig. 1(c). Lastly, the half-life of the (0_2^+) level in ^{70}Ni was determined by fitting the time-difference spectrum [Fig. 1(d)] generated by gating on the 307-keV, γ-ray region in the $LaBr_3$(Ce) detectors corresponding to the $(0_2^+) \rightarrow 2_1^+$ transition [11], resulting in a half-life of $t_{1/2} = 1.65^{+0.30}_{-0.25}$ ns.

In addition to measuring the half-life of the 0_3^+ state in ^{68}Ni, the first experimental observation of the 430-keV, $2_1^+ \rightarrow 0_2^+$ transition is reported. The $2_1^+ \rightarrow 0_2^+$ branching ratio in ^{68}Ni was determined in a separate experiment performed at the NSCL and described in Ref. [11]. Only the salient features are repeated here. Using the same primary and secondary beams, the ions were implanted 1 mm deep into a planar Germanium Double-Sided Strip Detector (GeDSSD) [33] and β-delayed γ rays were recorded using SeGA. The unique nature of the experimental signal resulting from the decay of the 0_2^+ isomeric state provided for a sensitive identification of transitions populating it [10], including the low-intensity, 430-keV transition. This γ-ray spectrum is presented in Fig. 2(a) and expanded around the 430-keV region in Fig. 2(b). After incorporating both the γ-ray and 0_2^+ isomer detection efficiencies, the absolute intensity of the 430-keV γ ray was determined upon comparison with that of the 2033-keV, $2_1^+ \rightarrow 0_1^+$ transition and resulted in a 0.12(3)% branch. Using the branching ratio and lifetime of the $2_1^+ \rightarrow 0_2^+$ transition in ^{68}Ni, the measured $B(E2: 2_1^+ \rightarrow 0_2^+)$ transition probability is 147(46) e^2fm^4.

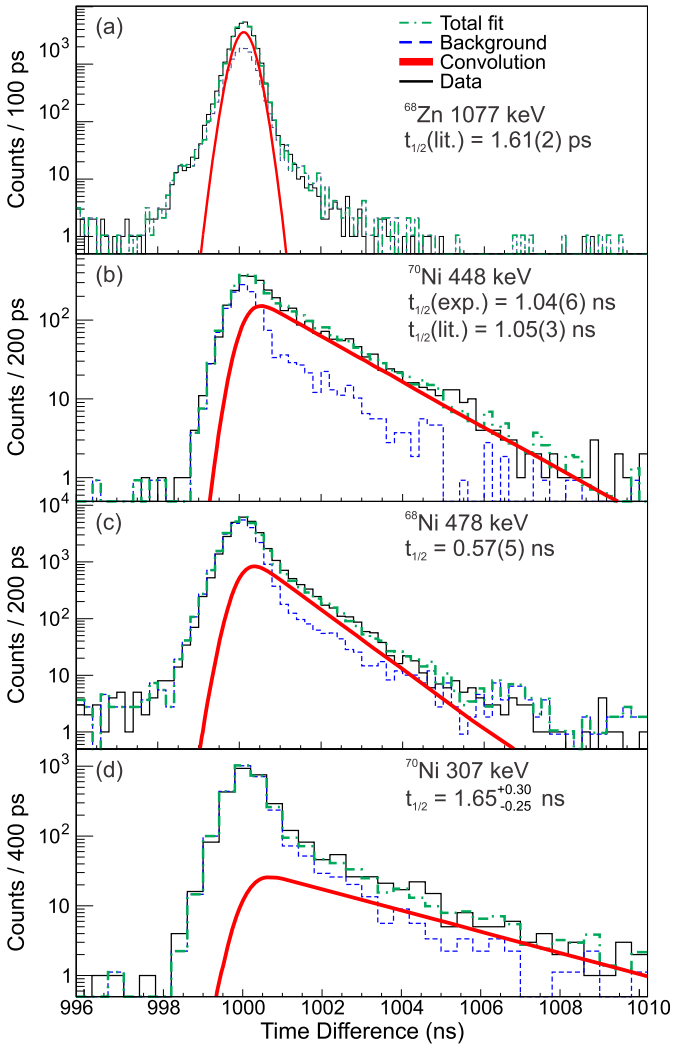

Fig. 1. (a) Time difference between the $LaBr_3(Ce)$ array and the implantation scintillator, arbitrarily offset by 1000 ns, illustrating the prompt response for the 1.61(2)-ps, 1077-keV, $2_1^+ \rightarrow 0_1^+$, ^{68}Zn transition. (b) Time difference gated on the 448-keV, $6^+ \rightarrow 4^+$ transition in ^{70}Ni. The curve was fit with a background sampled at an energy just less than the peak and a weighted linear combination of Gaussian detector responses convoluted with an exponential decay. (c) Time difference gated on the 478-keV, $0_3^+ \rightarrow 2_1^+$, ^{68}Ni transition. The background shown was sampled at an energy just less than the peak. (d) Time difference gated on the 307-keV $(0_2^+) \rightarrow 2_1^+$ ^{70}Ni transition. The background shown was sampled at an energy just greater than the region of interest.

An upper limit was placed on the intensity of the 907-keV, $0_3^+ \rightarrow 0_2^+$ $E0$ transition based on non-observation of the 1515-keV, $(2_3^+) \rightarrow 0_3^+$ transition in the spectrum of γ rays populating the 0_2^+ isomer [Fig. 2(c)]. An upper limit on the intensity of the 2511-keV, $0_3^+ \rightarrow 0_1^+$, $E0$ decay was based on the lack of a 1515-511-keV coincidence, where a 511-keV signal would originate from the internal pair-production decay of the 2511-keV, $0_3^+ \rightarrow 0_1^+$ transition. The intensity limits result in branching ratio limits of $BR_{907} < 0.0018$ and $BR_{2511} < 0.0173$. Limits on monopole transition strengths were determined using the level lifetimes and electronic factors from the BrIcc code [34]. The summed $E0$ branch out of the 0_3^+ state is consistent with the limit found in Ref. [16]. The branching ratios and half-life results are given in Table 1 and the low-energy level scheme summarizing the new experimental information is provided in Fig. 3.

Using a simple, two level mixing model with spherical and deformed unmixed states and assuming significant mixing only for the 0^+ states, information on the mixing and deformation difference between the 0_1^+ and 0_2^+ states in ^{68}Ni can be obtained using the relation $B(E2:2_1^+ \rightarrow 0_1^+)/B(E2:2_1^+ \rightarrow 0_2^+) \sim \tan^2\theta$ [36], where θ is the mixing angle. A previous experiment placed a limit of $\cos^2\theta > 0.7$ from complementary data on relative cross sections populating the 0_1^+ and 0_2^+ states in the ^{66}Ni(t,p)^{68}Ni reaction [37,38]. From the $B(E2)$ values of Fig. 3 and Table 1, a mixing amplitude of $\cos^2\theta = 0.74(7)$ is determined (for reference, in the case of maximal mixing $\cos^2\theta = 0.5$). While the work in Ref. [37] was unable to distinguish between values representing a strong mixing between the $p_{1/2}$ and $g_{9/2}$ orbits and those for a nearly closed-shell configuration, the present results clearly favor the mixed wave functions.

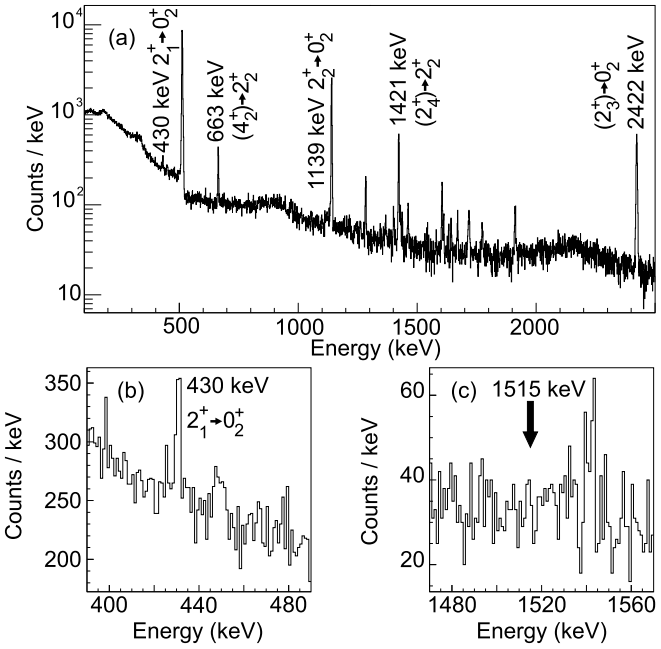

Fig. 2. γ-ray spectrum recorded in SeGA coincident with the ^{68}Ni $0_2^+ \rightarrow 0_1^+$ transition, (a) from 100 to 2500 keV, (b) around the 430-keV $2_1^+ \rightarrow 0_2^+$ transition, and (c) around 1515 keV, the location expected for the $(2_3^+) \rightarrow 0_3^+$ feeding transition.

The magnitude of the electric monopole matrix element can be written using the relationship $\rho^2(E0) = (Z^2/R_0^4)\cos^2\theta(1 - \cos^2\theta)[\Delta\langle r^2\rangle]^2$, where $\Delta\langle r^2\rangle$ is the difference in mean-square charge radii between states involved in the decay [42]. Using the known value $\rho^2(E0:0_2^+ \rightarrow 0_1^+) = 0.0076(4)$ [10] and the mixing angle calculated from this work, a difference in mean-square charge radii of 0.17(2) fm^2 was determined. Under the assumptions of a spherical 0_1^+ state and an axially symmetric deformation, an absolute value of the intrinsic quadrupole moment of 93(5) $e$fm^2 is obtained for the 0_2^+ state. This value is consistent with the prediction of -95 $e$fm^2 made earlier [10].

To appropriately describe the results in Fig. 3 and Table 1, theoretical calculations must simultaneously reproduce a large $B(E2:2_1^+ \rightarrow 0_2^+)$ value, a low 0_3^+ energy, and the measured 0_3^+ half-life in ^{68}Ni combined with the new 0_2^+ lifetime in ^{70}Ni. Numerous theoretical studies have been performed to understand structure in the vicinity of ^{68}Ni [19,21,22,43–45]. A significant dividing line between theoretical treatments is whether proton excitations across the $Z = 28$ gap are included. The JUN45 interaction (among others; see e.g. Ref. [10]) explicitly prohibits proton excitations and considers a model space containing the $f_{5/2}$, $p_{3/2}$, $p_{1/2}$, and $g_{9/2}$ neutron single-particle orbitals. The interaction is able to reproduce the energy of the 0_2^+ state in ^{68}Ni, as can calculations that use interactions developed in the larger $fpg_{9/2}d_{5/2}$ model space for protons

Table 1
Half-lives, branching ratios, and either absolute $B(E2)$ in $e^2\text{fm}^4$ or $\rho^2(E0)$, depending on the nature of the transition.

Nucleus	J_i^π	$t_{1/2}$	J_f^π	BR	$B(E2)$	$\rho^2(E0)$
^{68}Ni	0_2^+	268(12) ns[a]	0_1^+	1.0		0.0076(4)[a]
	2_1^+	0.31(5) ps[b]	0_1^+	$0.999^{+0.001}_{-0.05}$	52.5(84)	
			0_2^+	$1.2(3)\times10^{-3}$	147(46)	
	0_3^+	0.57(5) ns	0_1^+	<0.0173		<0.0050
			0_2^+	<0.0018		<0.0258
			2_1^+	>0.981	39.0(34)	
^{70}Ni	(0_2^+)	$1.65^{+0.30}_{-0.25}$ ns	2_1^+	>0.66	>58	
			0_1^+	<0.33		<0.54

[a] from Ref. [10].
[b] from Ref. [35].

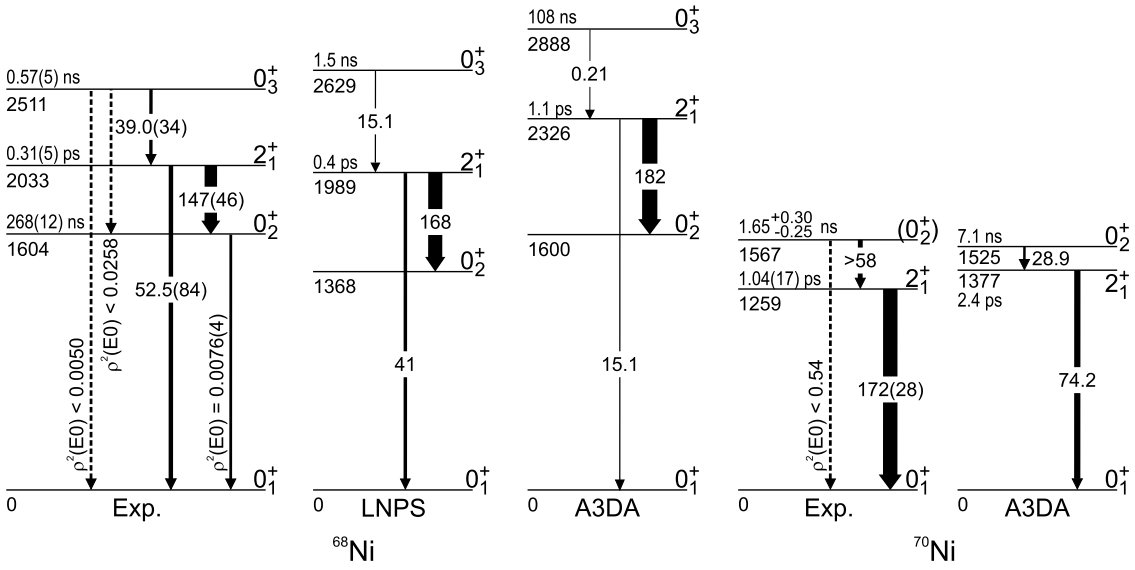

Fig. 3. Half-lives and transition strengths of the lowest four states in ^{68}Ni compared to theoretical predictions [16,39]. Half-lives of the states, where known, are given on the upper left side of each level with the associated energies (in keV) on the lower left side. Unobserved transitions are indicated by dotted lines. Electric monopole transition strengths are given for the $E0$ transitions. $B(E2)$ values are labeled in $e^2\text{fm}^4$. Experimental values for the ^{70}Ni, 2_1^+ state half-life and $B(E2)$ strength are adopted from Ref. [40]. Note that, while LNPS predictions of the ^{70}Ni $B(E2:0_2^+\rightarrow2_1^+)$ value have not been published so far, Ref. [41] indicates a calculated $B(E2:2_1^+\rightarrow0_1^+)$ value of 102 $e^2\text{fm}^4$ (not shown).

and neutrons, such as shell-model calculations using the LNPS effective interaction [22] and the Monte Carlo Shell Model (MCSM) using the A3DA interaction [19]. This is consistent with the interpretation of the 0_2^+ state as predominantly due to the excitation of a pair of neutrons across $N=40$ into the $\nu g_{9/2}$ orbital [10,15,16]. The difference between the model spaces is apparent in the energy of the 0_3^+ level, with only the newer, larger model spaces predicting its energy below 3 MeV. The wave function of this 0_3^+ state in ^{68}Ni is dominated by proton excitations across $Z=28$. The importance of proton excitations has also been demonstrated in the one-proton hole nuclei ^{65,67,69}Co [46–49] Along with the accurate reproduction of level energies, the LNPS and MCSM calculations further suggest shape coexistence in ^{68}Ni with each of the 0_1^+, 0_2^+, and 0_3^+ states associated with spherical, oblate, and prolate shapes, respectively [10,19,20].

The experimental data are compared to predicted lifetimes and $B(E2)$ strengths in Fig. 3 and Table 1. The 0_3^+ half life is predicted to be either 108 ns or 1.5 ns using the A3DA or LNPS effective interactions, respectively. The MCSM calculations overestimate the half-life while the LNPS ones provide the correct order of magnitude. For the half-life of the ^{70}Ni (0_2^+) level, the MCSM predicts a value of 7.2 ns [39]. This is better agreement than what is found for the ^{68}Ni 0_3^+ state. However, there is room for improvement within both the shell-model and MCSM frameworks to better reproduce the half-lives of these excited 0^+ states.

The $B(E2:2_1^+\rightarrow0_2^+)$ value in ^{68}Ni is consistent with either interaction (Fig. 3, Table 1) and provides strong experimental support for associating the 2_1^+ and 0_2^+ states with a similar configuration, as was previously discussed in Refs. [15,16]. For the $B(E2:0_3^+\rightarrow2_1^+)$ probability in ^{68}Ni, a 98.1% branching ratio was adopted while for the $B(E2:(0_2^+)\rightarrow2_1^+)$ probability in ^{70}Ni, a measured branching ratio limit of $>66\%$ corresponds to a lower limit (2σ) of >58 $e^2\text{fm}^4$. In order to determine an upper limit, the assumption of a 100% branch corresponds to a value of 128^{+24}_{-20} $e^2\text{fm}^4$. Both the $B(E2:(0_2^+)\rightarrow2_1^+)$ value in ^{70}Ni and $B(E2:0_3^+\rightarrow2_1^+)$ value in ^{68}Ni are similar in magnitude and both are above theoretical expectations (Fig. 3, Table 1). Unfortunately, there are no predictions of the electric monopole transition strengths at this time, and this remains an area for advancement of the theoretical description of this region.

These results constitute the first quantitative description of the first two 0^+ states in ^{68}Ni where the degree of mixing of nuclear

configurations with different mean square charge radii has been determined within a two-level mixing model without assuming maximal mixing, as was done in prior studies. When combined with the presented results on ^{70}Ni that find good agreement with MCSM calculations describing the depth of a prolate well alongside a spherical minimum, altogether these results settle the question of whether there is shape coexistence in the Ni nuclei comparable to that in Sn and Pb nuclei.

Shape coexistence has now been observed accompanying all proton closed shells at and above Ni ($Z = 28$) between neutron shell closures. As a result, the same phenomenon should be expected in more neutron-rich regions directly in the path of the r process, such as those centered on neutron-rich ^{154}Sn and ^{220}Pb. The nucleus ^{154}Sn is located on the low-mass side of the rare-earth peak that has received considerable attention as a possible distinguishing feature of r-process sites. Shape coexistence would significantly affect half-lives without substantially altering relative mass differences in these regions and could have an impact on the resulting abundance distributions [50]. Direct observation of shape coexistence in these nuclei is a considerable challenge, so the knowledge supplied from other regions where shape coexistence has been characterized is relevant to predicting the location and extent of deformation in the r-process path.

In summary, new half-life measurements of the 0_3^+ and (0_2^+) states in ^{68}Ni and ^{70}Ni, along with the measurement of the previously unobserved $2_1^+ \rightarrow 0_2^+$ branching ratio in ^{68}Ni, have allowed for the determination of many new electric dipole transition strengths as well as placed limits on electric monopole transition strengths. In particular, the ratio of $B(E2: 2_1^+ \rightarrow 0_2^+)$ and $B(E2: 2_1^+ \rightarrow 0_1^+)$ strengths in ^{68}Ni led to a mixing amplitude of 0.74(7) between a deformed excited state and a spherical ground state within a two-level mixing model. This determination enabled a fully quantitative calculation of the difference in mean-square radii of 0.17(2) fm^2; the first of its kind requiring no assumptions on the amount of mixing. The comparison of results to large-scale shell models validates the interpretation of shape coexistence through fully characterized experimental quantities.

Acknowledgements

This work was supported in part by the National Science Foundation (NSF) under Contract No. PHY-1102511 (NSCL) and Grant No. PHY-1350234 (CAREER), by the Department of Energy National Nuclear Security Administration (NNSA) under Grant No. DE-NA0002132 and Award No. DE-NA0003221 and through the Nuclear Science and Security Consortium under Award No's. DE-NA0000979 and DE-NA0003180, by the U.S. Department of Energy, Office of Science, Office of Nuclear Physics, under Contract No. DE-AC-06CH11357 (ANL) and Grant No's. DE-FG02-94ER40834 (Maryland) and DE-FG02-96ER40983 (UT), and by the U.S. Army Research Laboratory under Cooperative Agreement W911NF-12-2-0019.

References

[1] M.G. Mayer, Nuclear configurations in the spin-orbit coupling model. I. Empirical evidence, Phys. Rev. 78 (1950) 16–21, http://dx.doi.org/10.1103/PhysRev.78.16.

[2] K. Heyde, J.L. Wood, Shape coexistence in atomic nuclei, Rev. Mod. Phys. 83 (2011) 1467–1521, http://dx.doi.org/10.1103/RevModPhys.83.1467.

[3] A.N. Andreyev, M. Huyse, P. Van Duppen, L. Weissman, D. Ackermann, J. Gerl, F.P. Hessberger, S. Hofmann, A. Kleinbohl, G. Munzenberg, S. Reshitko, C. Schlegel, H. Schaffner, P. Cagarda, M. Matos, S. Saro, A. Keenan, C. Moore, C.D. O'Leary, R.D. Page, M. Taylor, H. Kettunen, M. Leino, A. Lavrentiev, R. Wyss, K. Heyde, A triplet of differently shaped spin-zero states in the atomic nucleus ^{186}Pb, Nature 405 (2000) 430, http://dx.doi.org/10.1038/35013012.

[4] W. Dietrich, A. Bäcklin, C.O. Lannergård, I. Ragnarsson, Possible rotational states in odd in nuclei, Nucl. Phys. A 253 (2) (1975) 429–447, http://dx.doi.org/10.1016/0375-9474(75)90490-X, http://www.sciencedirect.com/science/article/pii/037594747590490X.

[5] A. Bäcklin, B. Fogelberg, S.G. Malmskog, Possible deformed states in ^{115}In and ^{117}In, Nucl. Phys. A 96 (3) (1967) 539–560, http://dx.doi.org/10.1016/0375-9474(67)90604-5, http://www.sciencedirect.com/science/article/pii/0375947467906045.

[6] R.L. Auble, J.B. Ball, C.B. Fulmer, Levels in odd-mass Sb and I isotopes studied with the (^{3}He, d) reaction, Phys. Rev. 169 (1968) 955–962, http://dx.doi.org/10.1103/PhysRev.169.955.

[7] J. Bron, W.H.A. Hesselink, A.V. Poelgeest, J.J.A. Zalmstra, M.J. Uitzinger, H. Verheul, K. Heyde, M. Waroquier, H. Vincx, P.V. Isacker, Collective bands in even mass Sn isotopes, Nucl. Phys. A 318 (3) (1979) 335–351, http://dx.doi.org/10.1016/0375-9474(79)90653-5, http://www.sciencedirect.com/science/article/pii/0375947479906535.

[8] S.N. Liddick, S. Suchyta, B. Abromeit, A. Ayres, A. Bey, C.R. Bingham, M. Bolla, M.P. Carpenter, L. Cartegni, C.J. Chiara, H.L. Crawford, I.G. Darby, R. Grzywacz, G. Gürdal, S. Ilyushkin, N. Larson, M. Madurga, E.A. McCutchan, D. Miller, S. Padgett, S.V. Paulauskas, J. Pereira, M.M. Rajabali, K. Rykaczewski, S. Vinnikova, W.B. Walters, S. Zhu, Shape coexistence along $n = 40$, Phys. Rev. C 84 (2011) 061305, http://dx.doi.org/10.1103/PhysRevC.84.061305.

[9] M.P. Carpenter, R.V.F. Janssens, S. Zhu, Shape coexistence in neutron-rich nuclei near $n = 40$, Phys. Rev. C 87 (2013) 041305, http://dx.doi.org/10.1103/PhysRevC.87.041305.

[10] S. Suchyta, S.N. Liddick, Y. Tsunoda, T. Otsuka, M.B. Bennett, A. Chemey, M. Honma, N. Larson, C.J. Prokop, S.J. Quinn, N. Shimizu, A. Simon, A. Spyrou, V. Tripathi, Y. Utsuno, J.M. VonMoss, Shape coexistence in ^{68}Ni, Phys. Rev. C 89 (2014) 021301, http://dx.doi.org/10.1103/PhysRevC.89.021301.

[11] C.J. Prokop, B.P. Crider, S.N. Liddick, A.D. Ayangeakaa, M.P. Carpenter, J.J. Carroll, J. Chen, C.J. Chiara, H.M. David, A.C. Dombos, S. Go, J. Harker, R.V.F. Janssens, N. Larson, T. Lauritsen, R. Lewis, S.J. Quinn, F. Recchia, D. Seweryniak, A. Spyrou, S. Suchyta, W.B. Walters, S. Zhu, New low-energy 0^+ state and shape coexistence in ^{70}Ni, Phys. Rev. C 92 (2015) 061302(R), http://dx.doi.org/10.1103/PhysRevC.92.061302.

[12] C.J. Chiara, D. Weisshaar, R.V.F. Janssens, Y. Tsunoda, T. Otsuka, J.L. Harker, W.B. Walters, F. Recchia, M. Albers, M. Alcorta, V.M. Bader, T. Baugher, D. Bazin, J.S. Berryman, P.F. Bertone, C.M. Campbell, M.P. Carpenter, J. Chen, H.L. Crawford, H.M. David, D.T. Doherty, A. Gade, C.R. Hoffman, M. Honma, F.G. Kondev, A. Korichi, C. Langer, N. Larson, T. Lauritsen, S.N. Liddick, E. Lunderberg, A.O. Macchiavelli, S. Noji, C. Prokop, A.M. Rogers, D. Seweryniak, N. Shimizu, S.R. Stroberg, S. Suchyta, Y. Utsuno, S.J. Williams, K. Wimmer, S. Zhu, Identification of deformed intruder states in semi-magic ^{70}Ni, Phys. Rev. C 91 (2015) 044309, http://dx.doi.org/10.1103/PhysRevC.91.044309.

[13] J. Wood, K. Heyde, W. Nazarewicz, M. Huyse, P. van Duppen, Coexistence in even-mass nuclei, Physics Reports 215 (3) (1992) 101–201, http://dx.doi.org/10.1016/0370-1573(92)90095-H, http://www.sciencedirect.com/science/article/pii/037015739290095H.

[14] P. Sarriguren, A. Algora, J. Pereira, Gamow-teller response in deformed even and odd neutron-rich Zr and Mo isotopes, Phys. Rev. C 89 (2014) 034311, http://dx.doi.org/10.1103/PhysRevC.89.034311.

[15] F. Recchia, C.J. Chiara, R.V.F. Janssens, D. Weisshaar, A. Gade, W.B. Walters, M. Albers, M. Alcorta, V.M. Bader, T. Baugher, D. Bazin, J.S. Berryman, P.F. Bertone, B.A. Brown, C.M. Campbell, M.P. Carpenter, J. Chen, H.L. Crawford, H.M. David, D.T. Doherty, C.R. Hoffman, F.G. Kondev, A. Korichi, C. Langer, N. Larson, T. Lauritsen, S.N. Liddick, E. Lunderberg, A.O. Macchiavelli, S. Noji, C. Prokop, A.M. Rogers, D. Seweryniak, S.R. Stroberg, S. Suchyta, S. Williams, K. Wimmer, S. Zhu, Configuration mixing and relative transition rates between low-spin states in ^{68}Ni, Phys. Rev. C 88 (2013) 041302, http://dx.doi.org/10.1103/PhysRevC.88.041302.

[16] F. Flavigny, D. Pauwels, D. Radulov, I.J. Darby, H. De Witte, J. Diriken, D.V. Fedorov, V.N. Fedosseev, L.M. Fraile, M. Huyse, V.S. Ivanov, U. Köster, B.A. Marsh, T. Otsuka, L. Popescu, R. Raabe, M.D. Seliverstov, N. Shimizu, A.M. Sjödin, Y. Tsunoda, P. Van den Bergh, P. Van Duppen, J. Van de Walle, M. Venhart, W.B. Walters, K. Wimmer, Characterization of the low-lying 0^+ and 2^+ states in ^{68}Ni via β decay of the low-spin ^{68}Co isomer, Phys. Rev. C 91 (2015) 034310, http://dx.doi.org/10.1103/PhysRevC.91.034310.

[17] W.F. Mueller, B. Bruyneel, S. Franchoo, M. Huyse, J. Kurpeta, K. Kruglov, Y. Kudryavtsev, N.V.S.V. Prasad, R. Raabe, I. Reusen, P. Van Duppen, J. Van Roosbroeck, L. Vermeeren, L. Weissman, Z. Janas, M. Karny, T. Kszczot, A. Plochocki, K.-L. Kratz, B. Pfeiffer, H. Grawe, U. Köster, P. Thirolf, W.B. Walters, Phys. Rev. C 61 (2000) 054308, http://dx.doi.org/10.1103/PhysRevC.61.054308.

[18] C.J. Chiara, R. Broda, W.B. Walters, R.V.F. Janssens, M. Albers, M. Alcorta, P.F. Bertone, M.P. Carpenter, C.R. Hoffman, T. Lauritsen, A.M. Rogers, D. Seweryniak, S. Zhu, F.G. Kondev, B. Fornal, W. Królas, J. Wrzesiński, N. Larson, S.N. Liddick, C. Prokop, S. Suchyta, H.M. David, D.T. Doherty, Low-spin states and the non-observation of a proposed 2202-keV, 0^+ isomer in ^{68}Ni, Phys. Rev. C 86 (2012) 041304, http://dx.doi.org/10.1103/PhysRevC.86.041304.

[19] Y. Tsunoda, T. Otsuka, N. Shimizu, M. Honma, Y. Utsuno, Novel shape evolution in exotic Ni isotopes and configuration-dependent shell structure, Phys. Rev. C 89 (2014) 031301, http://dx.doi.org/10.1103/PhysRevC.89.031301.

[20] A. Poves, Shape coexistence: the shell model view, J. Phys. G Nucl. Part. Phys. 43 (2) (2016) 024010, http://stacks.iop.org/0954-3899/43/i=2/a=024010.

[21] M. Honma, T. Otsuka, T. Mizusaki, M. Hjorth-Jensen, New effective interaction for f_5pg_9-shell nuclei, Phys. Rev. C 80 (2009) 064323, http://dx.doi.org/10.1103/PhysRevC.80.064323.

[22] S.M. Lenzi, F. Nowacki, A. Poves, K. Sieja, Island of inversion around ^{64}Cr, Phys. Rev. C 82 (2010) 054301, http://dx.doi.org/10.1103/PhysRevC.82.054301.

[23] M. Girod, P. Dessagne, M. Bernas, M. Langevin, F. Pougheon, P. Roussel, Spectroscopy of neutron-rich nickel isotopes: Experimental results and microscopic interpretation, Phys. Rev. C 37 (1988) 2600–2612, http://dx.doi.org/10.1103/PhysRevC.37.2600.

[24] L. Gaudefroy, A. Obertelli, S. Péru, N. Pillet, S. Hilaire, J.P. Delaroche, M. Girod, J. Libert, Collective structure of the $n = 40$ isotones, Phys. Rev. C 80 (2009) 064313, http://dx.doi.org/10.1103/PhysRevC.80.064313.

[25] P. Möller, A. Sierk, R. Bengtsson, H. Sagawa, T. Ichikawa, Nuclear shape isomers, At. Data Nucl. Data Tables 98 (2) (2012) 149–300, http://dx.doi.org/10.1016/j.adt.2010.09.002, http://www.sciencedirect.com/science/article/pii/S0092640X11000477.

[26] D.J. Morrissey, B.M. Sherrill, M. Steiner, A. Stolz, I. Wiedenhoever, Commissioning the {A1900} projectile fragment separator, Nucl. Instrum. Methods Phys. Res. B 204 (0) (2003) 90–96, http://dx.doi.org/10.1016/S0168-583X(02)01895-5, 14th International Conference on Electromagnetic Isotope Separators and Techniques Related to their Applications, http://www.sciencedirect.com/science/article/pii/S0168583X02018955.

[27] M. Alshudifat, R. Grzywacz, S.V. Paulauskas, Development of a segmented scintillator for decay studies, Physics Procedia 66 (2015) 445–450.

[28] W.F. Mueller, J.A. Church, T. Glasmacher, D. Gutknecht, G. Hackman, P.G. Hansen, Z. Hu, K.L. Miller, P. Quirin, Thirty-two-fold segmented germanium detectors to identify g-rays from intermediate-energy exotic beams, Nucl. Instrum. Methods Phys. Res. A 466 (3) (2001) 492–498, http://dx.doi.org/10.1016/S0168-9002(01)00257-1, http://www.sciencedirect.com/science/article/pii/S0168900201002571.

[29] C.J. Prokop, S.N. Liddick, B.L. Abromeit, A.T. Chemey, N.R. Larson, S. Suchyta, J.R. Tompkins, Digital data acquisition system implementation at the national superconducting cyclotron laboratory, Nucl. Instrum. Methods Phys. Res. A 741 (0) (2014) 163–168, http://dx.doi.org/10.1016/j.nima.2013.12.044, http://www.sciencedirect.com/science/article/pii/S0168900213017488.

[30] S. Agostinelli, J. Allison, K. Amako, J. Apostolakis, H. Araujo, P. Arce, M. Asai, D. Axen, S. Banerjee, G. Barrand, F. Behner, L. Bellagamba, J. Boudreau, L. Broglia, A. Brunengo, H. Burkhardt, S. Chauvie, J. Chuma, R. Chytracek, G. Cooperman, G. Cosmo, P. Degtyarenko, A. Dell'Acqua, G. Depaola, D. Dietrich, R. Enami, A. Feliciello, C. Ferguson, H. Fesefeldt, G. Folger, F. Foppiano, A. Forti, S. Garelli, S. Giani, R. Giannitrapani, D. Gibin, J.J.G. Cadenas, I. Gonzlez, G.G. Abril, G. Greeniaus, W. Greiner, V. Grichine, A. Grossheim, S. Guatelli, P. Gumplinger, R. Hamatsu, K. Hashimoto, H. Hasui, A. Heikkinen, A. Howard, V. Ivanchenko, A. Johnson, F.W. Jones, J. Kallenbach, N. Kanaya, M. Kawabata, Y. Kawabata, M. Kawaguti, S. Kelner, P. Kent, A. Kimura, T. Kodama, R. Kokoulin, M. Kossov, H. Kurashige, E. Lamanna, T. Lampn, V. Lara, V. Lefebure, F. Lei, M. Liendl, W. Lockman, F. Longo, S. Magni, M. Maire, E. Medernach, K. Minamimoto, P.M. de Freitas, Y. Morita, K. Murakami, et al., Geant4a simulation toolkit, Nucl. Instrum. Methods Phys. Res. A 506 (3) (2003) 250–303, http://dx.doi.org/10.1016/S0168-9002(03)01368-8, http://www.sciencedirect.com/science/article/pii/S0168900203013688.

[31] C.J. Prokop, B.P. Crider, S.N. Liddick, M. Alshudifiat, A.D. Ayangeakaa, M.P. Carpenter, J.J. Carroll, J. Chen, C.J. Chiara, H.M. David, S. Go, R. Grzywacz, J. Harker, R.V.F. Janssens, T. Lauritsen, D. Seweryniak, W.B. Walters, S. Zhu, New method for level-lifetime measurements with thick scintillators (in prep.).

[32] H. Mach, M. Lewitowicz, M. Stanoiu, F. Becker, J. Blomqvist, M.J.G. Berge, R. Boutami, B. Cederwall, Z. Dlouhy, B. Fogelberg, L.M. Fraile, G. Georgiev, H. Grawe, R. Grzywacz, P.I. Johansson, W. Klamra, S. Lukyanov, M. Mineva, J. Mrazek, G. Neyens, F. de Oliveir Santos, M. Pfüzner, Y.E. Penionzhkevich, E. Ramström, M. Sawicka, Coupling of valence particles/holes to ^{68,70}Ni studied via measurements of the B(E2) strength in ^{67,69,70}Ni and ^{71}Cu, Nuclear Physics A 719 (2003) C213–C216, http://dx.doi.org/10.1016/S0375-9474(03)00920-5, http://www.sciencedirect.com/science/article/pii/S0375947403009205.

[33] N. Larson, S.N. Liddick, M. Bennett, A. Bowe, A. Chemey, C. Prokop, A. Simon, A. Spyrou, S. Suchyta, S.J. Quinn, S.L. Tabor, P. Tai, V. Tripathi, J.M. VonMoss, High efficiency beta-decay spectroscopy using a planar germanium double-sided strip detector, Nucl. Instrum. Methods Phys. Res. A 727 (0) (2013) 59–64, http://dx.doi.org/10.1016/j.nima.2013.06.027, http://www.sciencedirect.com/science/article/pii/S0168900213008474.

[34] T. Kibédi, T.W. Burrows, M.B. Trzhaskovskaya, P.M. Davidson, C.W. Nestor Jr., Evaluation of theoretical conversion coefficients using bricc, Nucl. Instrum. Methods Phys. Res. A 589 (2) (2008) 202–229, http://dx.doi.org/10.1016/j.nima.2008.02.051, http://www.sciencedirect.com/science/article/pii/S0168900208002520.

[35] E. McCutchan, Nuclear data sheets for $a = 68$, Nuclear Data Sheets 113 (67) (2012) 1735–1870, http://dx.doi.org/10.1016/j.nds.2012.06.002, http://www.sciencedirect.com/science/article/pii/S009037521200049X.

[36] H. Mach, M. Moszyński, R.L. Gill, F.K. Wohn, J.A. Winger, J.C. Hill, G. Molnár, K. Sistemich, Deformation and shape coexistence of 0^+ states in ^{98}Sr and ^{100}Zr, Physics Letters B 230 (1,2) (1989) 21–26, http://dx.doi.org/10.1016/0370-2693(89)91646-8, http://www.sciencedirect.com/science/article/pii/0370269389916468.

[37] J. Elseviers, Probing the semi-magicity of ^{68}Ni via the ^{66}Ni(t,p)^{68}Ni two-neutron transfer reaction in inverse kinematics, Ph.D. thesis, 2014, KU Leuven.

[38] J.A. Lay, L. Fortunato, A. Vitturi, Investigating nuclear pairing correlations via microscopic two-particle transfer reactions: The cases of ^{112}Sn, ^{32}Mg, and ^{68}Ni, Phys. Rev. C 89 (2014) 034618, http://dx.doi.org/10.1103/PhysRevC.89.034618.

[39] T. Otsuka, private communication.

[40] O. Perru, O. Sorlin, S. Franchoo, F. Azaiez, E. Bouchez, C. Bourgeois, A. Chatillon, J.M. Daugas, Z. Dlouhy, Z. Dombrádi, C. Donzaud, L. Gaudefroy, H. Grawe, S. Grévy, D. Guillemaud-Mueller, F. Hammache, F. Ibrahim, Y. Le Coz, S.M. Lukyanov, I. Matea, J. Mrazek, F. Nowacki, Y.-E. Penionzhkevich, F. de Oliveira Santos, F. Pougheon, M.G. Saint-Laurent, G. Sletten, M. Stanoiu, C. Stodel, C. Theisen, D. Verney, Enhanced core polarization in ^{70}Ni and ^{74}Zn, Phys. Rev. Lett. 96 (2006) 232501, http://dx.doi.org/10.1103/PhysRevLett.96.232501.

[41] K. Kolos, D. Miller, R. Grzywacz, H. Iwasaki, M. Al-Shudifat, D. Bazin, C.R. Bingham, T. Braunroth, G. Cerizza, A. Gade, A. Lemasson, S.N. Liddick, M. Madurga, C. Morse, M. Portillo, M.M. Rajabali, F. Recchia, L.L. Riedinger, P. Voss, W.B. Walters, D. Weisshaar, K. Whitmore, K. Wimmer, J.A. Tostevin, Direct lifetime measurements of the excited states in ^{72}Ni, Phys. Rev. Lett. 116 (2016) 122502, http://dx.doi.org/10.1103/PhysRevLett.116.122502.

[42] J. Wood, E. Zganjar, C.D. Coster, K. Heyde, Electric monopole transitions from low energy excitations in nuclei, Nuclear Physics A 651 (4) (1999) 323–368, http://dx.doi.org/10.1016/S0375-9474(99)00143-8, http://www.sciencedirect.com/science/article/pii/S0375947499001438.

[43] A.F. Lisetskiy, B.A. Brown, M. Horoi, H. Grawe, New $t = 1$ effective interactions for the $f_{5/2}p_{3/2}p_{1/2}g_{9/2}$ model space: Implications for valence-mirror symmetry and seniority isomers, Phys. Rev. C 70 (2004) 044314, http://dx.doi.org/10.1103/PhysRevC.70.044314.

[44] B. Cheal, E. Mané, J. Billowes, M.L. Bissell, K. Blaum, B.A. Brown, F.C. Charlwood, K.T. Flanagan, D.H. Forest, C. Geppert, M. Honma, A. Jokinen, M. Kowalska, A. Krieger, J. Krämer, I.D. Moore, R. Neugart, G. Neyens, W. Nörtershäuser, M. Schug, H.H. Stroke, P. Vingerhoets, D.T. Yordanov, M. Žáková, Nuclear spins and moments of ga isotopes reveal sudden structural changes between $n = 40$ and $n = 50$, Phys. Rev. Lett. 104 (2010) 252502, http://dx.doi.org/10.1103/PhysRevLett.104.252502.

[45] N. Shimizu, T. Abe, Y. Tsunoda, Y. Utsuno, T. Yoshida, T. Mizusaki, M. Honma, T. Otsuka, New-generation monte carlo shell model for the k computer era, Prog. Theor. Exp. Phys. 2012 (1) (2012) 01A205, http://dx.doi.org/10.1093/ptep/pts012.

[46] D. Pauwels, O. Ivanov, N. Bree, J. Büscher, T.E. Cocolios, J. Gentens, M. Huyse, A. Korgul, Y. Kudryavtsev, R. Raabe, M. Sawicka, I. Stefanescu, J. Van de Walle, P. Van den Bergh, P. Van Duppen, W.B. Walters, Shape isomerism at $N = 40$: Discovery of a proton intruder state in ^{67}Co, Phys. Rev. C 78 (4) (2008) 041307, http://dx.doi.org/10.1103/PhysRevC.78.041307.

[47] D. Pauwels, O. Ivanov, N. Bree, J. Büscher, T.E. Cocolios, M. Huyse, Y. Kudryavtsev, R. Raabe, M. Sawicka, J. Van de Walle, P. Van Duppen, A. Korgul, I. Stefanescu, A.A. Hecht, N. Hoteling, A. Wöhr, W.B. Walters, R. Broda, B. Fornal, W. Krolas, T. Pawlat, J. Wrzesinski, M.P. Carpenter, R.V.F. Janssens, T. Lauritsen, D. Seweryniak, S. Zhu, J.R. Stone, X. Wang, Structure of ^{65,67}Co studied through the β decay of ^{65,67}Fe and a deep-inelastic reaction, Phys. Rev. C 79 (4) (2009) 044309, http://dx.doi.org/10.1103/PhysRevC.79.044309.

[48] S.N. Liddick, W.B. Walters, C.J. Chiara, R.V.F. Janssens, B. Abromeit, A. Ayres, A. Bey, C.R. Bingham, M.P. Carpenter, L. Cartegni, J. Chen, H.L. Crawford, I.G. Darby, R. Grzywacz, J. Harker, C.R. Hoffman, S. Ilyushkin, F.G. Kondev, N. Larson, M. Madurga, D. Miller, S. Padgett, S.V. Paulauskas, M.M. Rajabali, K. Rykaczewski, D. Seweryniak, S. Suchyta, S. Zhu, Analogous intruder behavior near Ni, Sn, and Pb isotopes, Phys. Rev. C 92 (2015) 024319, http://dx.doi.org/10.1103/PhysRevC.92.024319.

[49] F. Recchia, S.M. Lenzi, S. Lunardi, E. Farnea, A. Gadea, N. Mărginean, D.R. Napoli, F. Nowacki, A. Poves, J.J. Valiente-Dobón, M. Axiotis, S. Aydin, D. Bazzacco, G. Benzoni, P.G. Bizzeti, A.M. Bizzeti-Sona, A. Bracco, D. Bucurescu, E. Caurier, L. Corradi, G. de Angelis, F. Della Vedova, E. Fioretto, A. Gottardo, M. Ionescu-Bujor, A. Iordachescu, S. Leoni, R. Mărginean, P. Mason, R. Menegazzo, D. Mengoni, B. Million, G. Montagnoli, R. Orlandi, G. Pollarolo, E. Sahin, F. Scarlassara, R.P. Singh, A.M. Stefanini, S. Szilner, C.A. Ur, O. Wieland, Spectroscopy of odd-mass cobalt isotopes toward the $n = 40$ subshell closure and shell-model description of spherical and deformed states, Phys. Rev. C 85 (2012) 064305, http://dx.doi.org/10.1103/PhysRevC.85.064305.

[50] M.R. Mumpower, G.C. McLaughlin, R. Surman, Formation of the rare-earth peak: Gaining insight into late-time r-process dynamics, Phys. Rev. C 85 (2012) 045801, http://dx.doi.org/10.1103/PhysRevC.85.045801.